Reactive Power Impacts on LCL Filter Capacitor Lifetime and Reliability in DFIG Grid-Connected Inverter

Zhou, Dao; Wang, Huai; Blaabjerg, Frede

Published in:
Proceedings of the IEEE Energy Conversion Congress and Exposition (ECCE 2018)

DOI (link to publication from Publisher):
10.1109/ECCE.2018.8558156

Publication date:
2018

Document Version
Accepted author manuscript, peer reviewed version

Reactive Power Impacts on LCL Filter Capacitor Lifetime and Reliability in DFIG Grid-connected Inverter

Dao Zhou, Huai Wang, and Frede Blaabjerg

Department of Energy Technology
Aalborg University, Aalborg, Denmark
zda@et.aau.dk; hwa@et.aau.dk; fbl@et.aau.dk

***Abstract* - With the increasing penetration of renewable power, its reliable and cost-effective production is of more and more importance. A filter is normally inserted between the grid-connected inverter and the power grid to reduce the PWM switching harmonics. According to an electro-thermal stress evaluation, the time-to-failure distribution of the single LCL filter capacitor is investigated in detail. Aiming at the system-level reliability analysis, a Weibull distribution based component-level individual capacitor can be linked together by using the reliability block diagram. A case study of a 2 MW wind power converter shows that the lifetime is significantly reduced from the individual capacitor to the capacitor bank. Besides, the over-excited reactive power injection further reduces the lifetime of the LCL filter capacitors.**

I. INTRODUCTION

Reliability and robustness of the system are closely related to its mission profile - the representation of all relevant conditions that the system will be exposed to in all of its intended application throughout its entire life cycle [1]. Then the failure may happen during the violation and overlap of the strength and stress distribution, in which the stressor factors may appear due to the environmental loads (like thermal, mechanical, humidity, etc.), or the functional loads (such as user profiles, electrical operation) [2].

The performance of power capacitor is complicated and highly affected by its operation conditions such as the voltage, current, frequency, and temperature. Many researchers have investigated the degradation of the electrolytic capacitors [3]-[5]. For instance, a real-time failure detection method is developed for the changes in the ESR and capacitance of the capacitors [3]. Lifetime prediction models of electrolytic capacitors are established for the switch-mode power supplies and variable-frequency drivers [4], [5]. However, few studies investigate the degradation effect on reliability evaluation considering the mission profile [6], and this paper develops the approach to evaluate the reliability of the metalized film capacitor featured as the filter. Moreover, it is a physics-of-failure approach [7] from the component-level to system-level reliability that integrates the electrical modeling, thermal modeling, Weibull distribution, and reliability block diagram.

This paper addresses the reliability assessment of the capacitors in a grid-connected inverter. Section II describes the design and failure mechanism of the filter capacitor. Reactive power impact on electrical stresses of the filter capacitor is presented in Section III. According to the mission profile based lifetime estimation of the individual capacitor, Section IV investigates and compares the time-to-failure from the capacitor cell to the capacitor bank. Finally, the concluding remarks are drawn in the last section.

II. DESIGN OF LCL FILTER CAPACITOR

As shown in Fig. 1(a), due to lots of switching harmonic voltage introduced by the Pulse Width Modulation (PWM) inverter, a filter is normally applied in between to mitigate the corresponding harmonic current flowing into the grid [8]. Since the renewable power generation systems are normally installed in remote areas, the PWM inverter is required to potentially provide or absorb the reactive power to support the grid voltage regulation. The reactive power profile specified in the German grid codes is shown in Fig. 1(b) [9], it is noted that different amounts of the Over-Excited (OE) and Under-Excited (UE) reactive power are required along with the various active power production.

As the LCL filter features as higher impedance at switching-frequency range compared to the single L filter, it generally is a preferred solution used in the grid-connected inverter. The design procedure of the LCL filter is well described in [10], the inverter-side inductor is selected according to the current switching ripple requirement, while the grid-side inductor is chosen on the basis of the harmonic specification from the IEEE standard. For the filter capacitor, it is designed seen from the additional introduced reactive power. As larger capacitance causes higher current stress of the power device and higher loss dissipation, 5%-10% of the absorbed reactive power at the rated operation condition is the rule-of-thumb [10].

It is well known that various types of the power capacitors are used in inverters. Electrolytic capacitors are applied in the case of high capacitance per volume (e.g. DC-link applications). Due to its low withstand voltage as well as the polarity, the metalized film capacitors are used in the grid

filter due to the high electric-field stress. Moreover, the material of polypropylene (PP) is preferred compared to polyethylene terephthalate (PET) because of the much lower loss factor. One of the main failure modes is often due to high capacitor temperature caused by the high current, which leads to a reduction of the breakdown voltage and even melting of the capacitor.

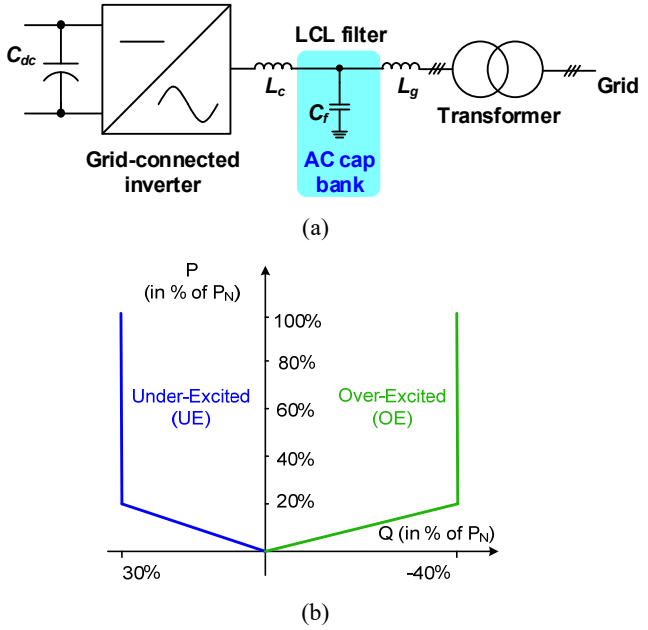

Fig. 1. Grid-connected inverter with LCL filter. (a) Configuration; (b) Reactive power requirement from German grid codes.

III. Reactive Power Impact on Capacitor Electrical Stresses

Based on the modulation scheme of the power converter, this section starts to analyze electrical stresses (e.g. the flowing current, and across voltage) of the filter capacitor with the help of the LCL filter impedance characteristics. In the wind power generation, the loading condition and reactive current impacts on capacitor electrical stresses are investigated and evaluated for the grid-connected power converter.

A. Electrical stresses of filter capacitor

To fully utilize the DC-link voltage, the Space Vector Modulation (SVM) is normally preferred in the three-phase system. As shown in Fig. 2(a), six sectors (Sector I to VI) can be divided in accordance with the phase angle of the output voltage φ_u. In the case of the Sector I, the voltage vector V_o is generally composed of two adjacent active vectors V_1 (100) and V_2 (110) (with duration periods of T_1 and T_2 within the switching period T_s), as well as two zero vectors V_0 (000) and V_7 (111) (with duration period of T_0 within the switching period T_s). Both the active and zero vectors are arranged symmetrically in order to achieve the minimum harmonics of the output voltage [11]. The possible switching patterns of the power devices are described in Fig. 2(b) in detail, where the active vectors V_1 and V_2, as well as zero vectors V_0 and V_7 are

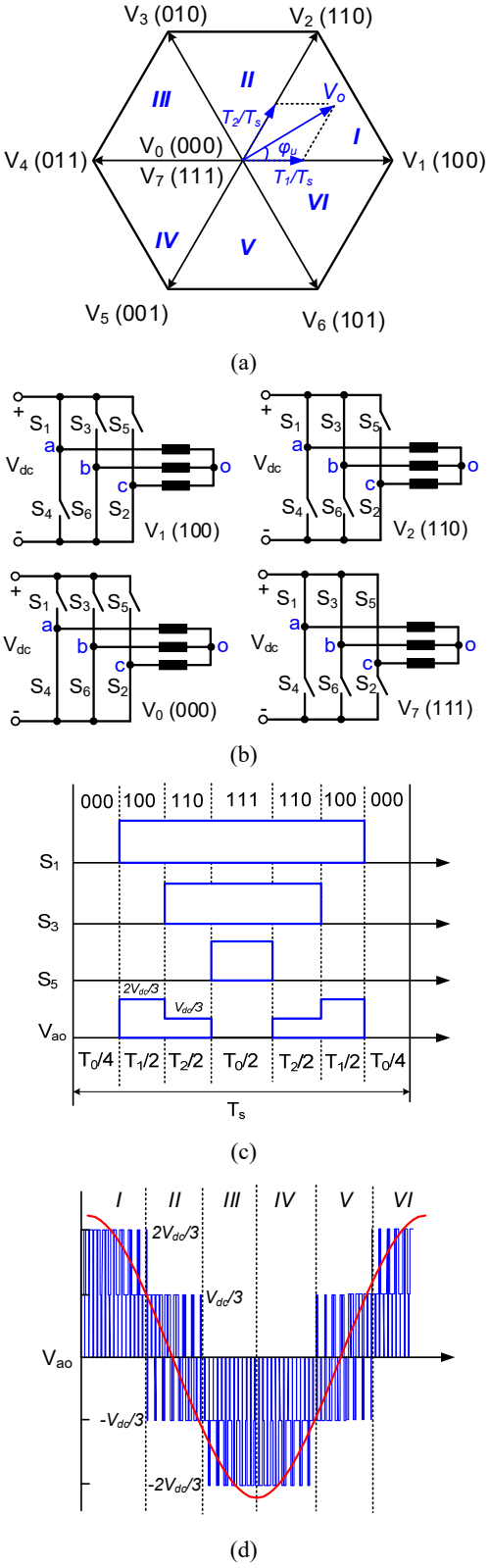

Fig. 2. Illustration of space vector modulation. (a) Six sectors. (b) Switching states existed in Sector I. (c) Phase voltage of converter output in Sector I. (d) Phase voltage of converter output within a fundamental period.

applied. Due to the symmetrical loading of the three-phase system, the inverter phase voltage V_{ao} is illustrated in Fig. 2(c). Depending on various switching states of the power devices, it can be seen that the output voltage includes the levels of $2V_{dc}/3$, $V_{dc}/3$, and 0, where the V_{dc} is the DC-link voltage. By using the similar approach, the voltage waveform of the inverter output can be expected in the other five sectors, which is consisted of three voltage levels within the same sector as described in Fig. 2(d).

Based on the position of the voltage vector, the duty cycle of active vectors d_1, d_2 and zero vector d_0 can be calculated in the following,

$$\begin{cases} d_1 = \dfrac{\sqrt{3}}{2} M \sin(\dfrac{k\pi}{3} - \varphi_u) \\ d_2 = \dfrac{\sqrt{3}}{2} M \sin(\varphi_u - \dfrac{(k-1)\pi}{3}) \\ d_0 = 1 - d_1 - d_2 \end{cases} \quad (1)$$

where k denotes the section number; M denotes the modulation index, which equals the peak value of the inverter voltage over the half of the DC-link voltage V_{dc} ($0 \leqslant M \leqslant 1.15$); φ_u denotes the phase angle of the inverter voltage.

For the LCL filter, it is well known that the majority of the harmonic current goes through the capacitor branch, while the fundamental current flows into the power grid to achieve high power quality. In order to calculate the harmonic components of the filter capacitor current and voltage, it is necessary to perform the Fourier analysis, which starts with the analysis of the converter voltage. For a pulse voltage, the Fourier coefficients can be calculated by its starting and ending time instants together with its voltage amplitude. Since there are 7 pulse voltages within a switching period as shown in Fig. 2(c), the Fourier coefficients can be simply accumulated from a single pulse voltage with the duty cycle as calculated in (1). With the information of voltage amplitude in various sectors as shown in Fig. 2(d), the Fourier coefficients can further be accumulated from a single switching period to the entire fundamental period. Thereafter, the harmonic components of the converter voltage can be deduced.

Table I

PARAMETERS OF 2 MW DFIG SYSTEM

Rated power	2 MW
Rated amplitude of phase voltage	563 V
Grid-side inductor	125 μH
Converter-side inductor	125 μH
Filter capacitor	300 μF
DC-link voltage	1050 V
Switching frequency	2 kHz

The relationship between the converter voltage and filter capacitor electrical stresses is tightly dependent on the characteristics of the LCL filter. With the parameters of the LCL filter used in 2 MW Doubly-Fed Induction Generator (DFIG) based wind turbine system listed in Table I, the transfer functions from the converter voltage to the capacitor current and voltage are respectively shown in Fig. 3. In the range above the switching frequency (40th order harmonic), both the capacitor current and voltage are weaken compared with the converter voltage.

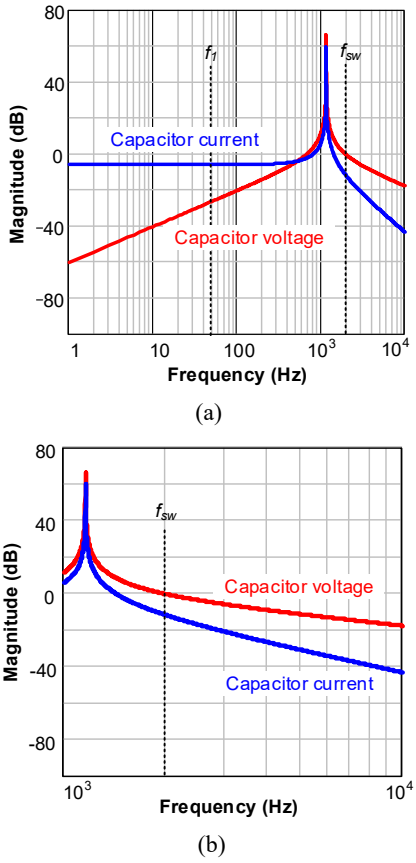

Fig. 3. LCL filter characteristic from converter voltage to filter capacitor voltage and current. (a) Overview. (b) Zoom-in area above switching frequency.

It is worthwhile to mention that due to the existence of the grid voltage and controller of the converter current, the relationship between the converter voltage u_c and capacitor current and voltage does not obey the transfer function as shown in Fig. 3. Since the impedance of the filter capacitor C_f is significantly higher than the grid-side inductor L_g at the fundamental frequency, the fundamental component of the converter current i_{g1} directly flows into the power grid, and the harmonic components go through the filter capacitor. Consequently, the filter capacitor can be considered as the open-circuit as shown in Fig. 4(a). In the case of the super-synchronous operation, the d-axis component of the grid current i_{gd1} becomes negative in order to provide the slip power from the induction generator into the power grid. Nevertheless, as shown in Fig. 4(b) and (c), the OE and UE reactive power injection make the q-axis component of the grid current i_{gq1} positive and negative, respectively. As the voltage drop across the filter inductor u_{L1} leads the converter

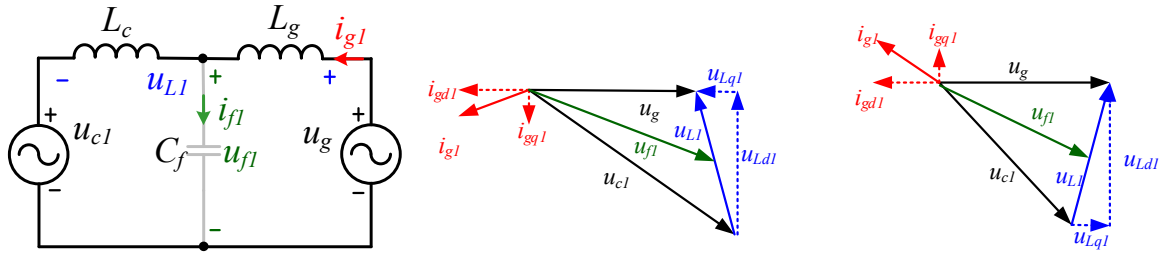

(a) (b) (c)

Fig. 4. Relationship between the converter voltage and the filter capacitor electrical stresses in the case of the fundamental frequency. (a) Configuration of the LCL filter. (b) Vector diagram of the LCL filter in the case of the over-excited reactive power injection. (c) Vector diagram of the LCL filter in the case of the under-excited reactive power injection.

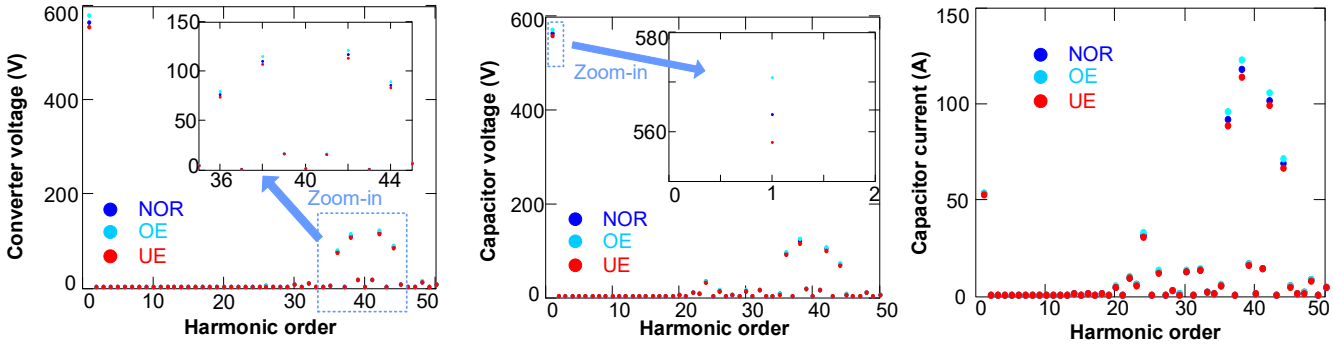

(a) (b) (c)

Fig. 5. Reactive power effects on harmonic spectrum of filter capacitor voltage and current at rated wind speed. (a) Converter voltage. (b) Capacitor voltage. (c) Capacitor current.

current 90°, its d-axis component u_{Ld1} is orthogonal to the grid voltage u_g, while its d-axis component u_{Ld1} is in the same or opposite direction with the grid voltage. It can be expected that the current reference at the q-axis affects more on the amplitude of the converter voltage. Since the voltage drop across the converter-side inductor L_c and the grid-side inductor is proportional to their inductance, the capacitor voltage can thereby be estimated. It is evident that the OE reactive power injection keeps the capacitor voltage higher than the power grid, while the UE reactive power injection makes the capacitor voltage lower than the power grid.

At the rated power of the DFIG operation, the harmonic spectrum of the capacitor voltage and current are shown in Fig. 5. To analyze the converter voltage, the Fourier coefficient is accumulated from a single pulse to the whole fundamental period. It can be seen that, apart from the required fundamental voltage produced by the controlled grid current, the harmonic components of the converter voltage is dominant by the harmonic orders around the switching frequency. Then, the voltage and current harmonic spectrum of the filter capacitor can be investigated based on the aforementioned transfer function. In the case of the NOR condition, it can be seen the fundamental component of the capacitor voltage is similar to the grid voltage, due to the small part of the orthogonal voltage drop across the filter capacitor compared to the grid voltage. In the case of reactive power operation, it is

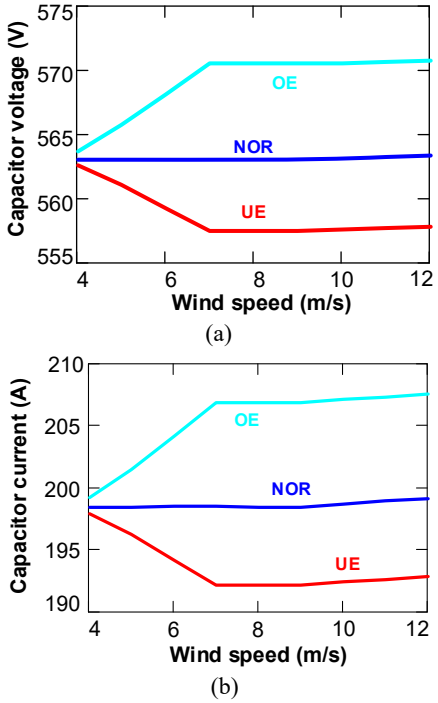

(a) (b)

Fig. 6. Electrical stresses of LCL filter capacitor with various wind speeds. (a) Fundamental component of capacitor voltage. (b) Harmonic components of capacitor current.

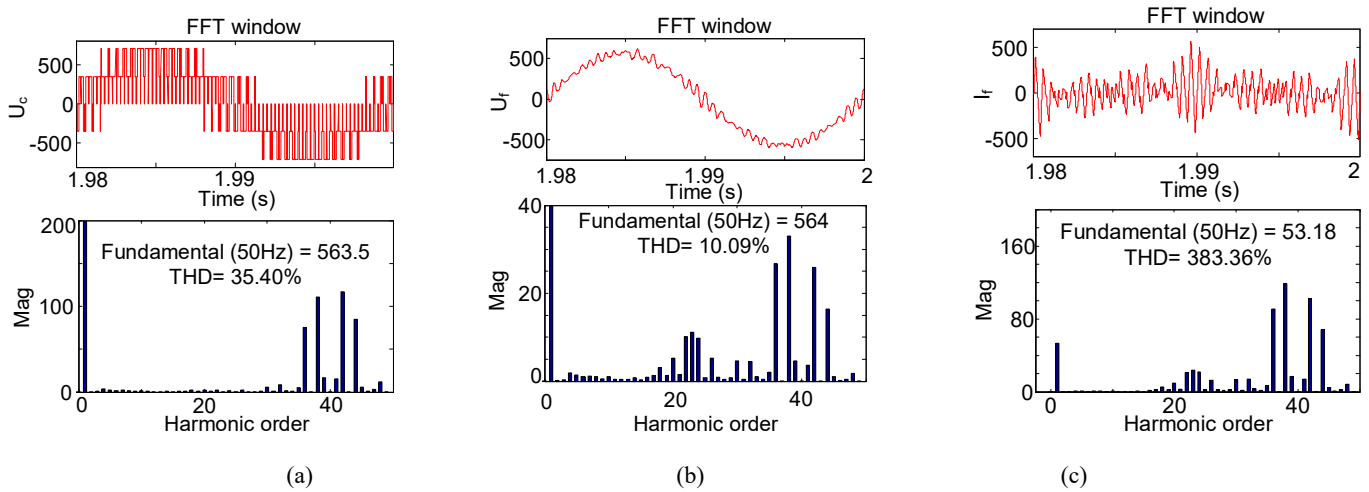

(a) (b) (c)

Fig. 7. Harmonic spectrum of filter voltage and current at rated wind speed with unity power factor. (a) Converter voltage. (b) Capacitor voltage. (c) Capacitor current.

noted that the fundamental component of the capacitor voltage increases under the OE reactive power but decreases under the UE reactive power. Similarly, the OE reactive power injection increases the harmonic components of the capacitor voltage, while the UE reactive power injection decreases the harmonic components of the capacitor voltage. In general, the fundamental component is significantly higher than the harmonic components in the converter and capacitor voltage. Nevertheless, the harmonic spectrum of the capacitor current is dominant by the harmonic components as shown in Fig. 5(c). In addition, it is evident that harmonic order around 23rd harmonic is amplified compared to the converter voltage due to the resonant frequency of the LCL filter.

According to the relationship between the wind speed and generator output power [12], together with the reactive power profile as shown in Fig. 1(b), the electrical stresses of the filter capacitor can be calculated from the cut-in wind speed of 4 m/s to the rated wind speed of 12 m/s. As the fundamental component dominates the capacitor voltage, while the harmonic components determine the capacitor current, both of them are in focus as shown in Fig. 6. It can be seen that the OE reactive power increases the current and voltage stresses, while the UE reactive power relieves the electrical stresses throughout the whole operation conditions.

B. Simulation validation

In order to verify the aforementioned analytical approach for the LCL filter capacitor electrical stresses, the capacitor voltage and current are investigated in the simulation with the focus on reactive power and loading impacts. The control strategy of 2 MW DFIG back-to-back power converter is the conventional vector control applied under the rotating reference frame.

In the case of the rated power and no reactive power injection, the simulated converter voltage, capacitor voltage, and capacitor current are shown in Fig. 8. Both the fundamental and harmonic components of the converter

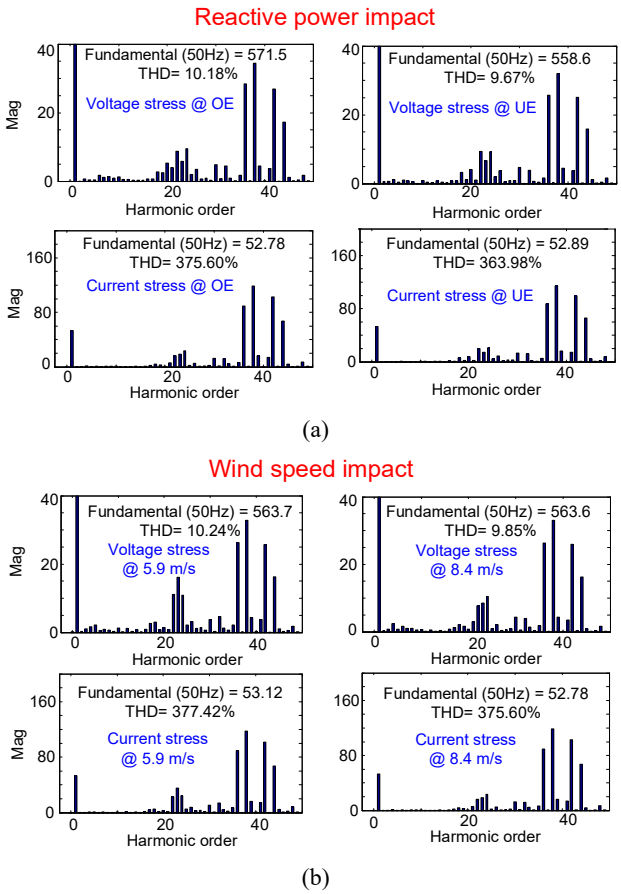

Fig. 8. Harmonic spectrum of capacitor voltage and current at various operation modes. (a) Impacts of reactive power at the rated wind speed. (b) Impacts of wind speeds with unity power factor.

voltage totally agree with the theoretical analysis, where the voltage harmonic components are mostly dominated sideband of the PWM switching. Apart from the fundamental and PWM switching harmonic component in the capacitor voltage, the harmonic components around 23rd order can be observed as well due to the resonant frequency of the LCL filter.

Moreover, it can be seen that the fundamental component is much higher than the PWM switching harmonic. Nevertheless, the switching harmonics of the capacitor current is more important.

The reactive power and loading impacts on the electrical stresses of the capacitor are shown in the Fig. 9(a) and (b), respectively. Regardless of the operation modes, it can be seen that the fundamental component dominates the capacitor voltage, while the harmonic components determine the capacitor current. In addition, it is evident that the fundamental component of the capacitor voltage slightly increases in the case of the OE reactive power, while it decreases a little in the case of the UE reactive power. Besides, the loading impacts on the electrical stresses are evaluated in the case of the unity power factor. As shown in Fig. 8(b), it can be evident that both the voltage and current of the capacitor almost keep the same.

IV. TIME-TO-FAILURE AND RELIABILITY OF FILTER CAPACITOR BANK

In this section, the lifetime of the individual capacitor can be converted into its corresponding time-to-failure. Then, the reliability evaluation of the capacitor bank can be analyzed by using the reliability block diagram.

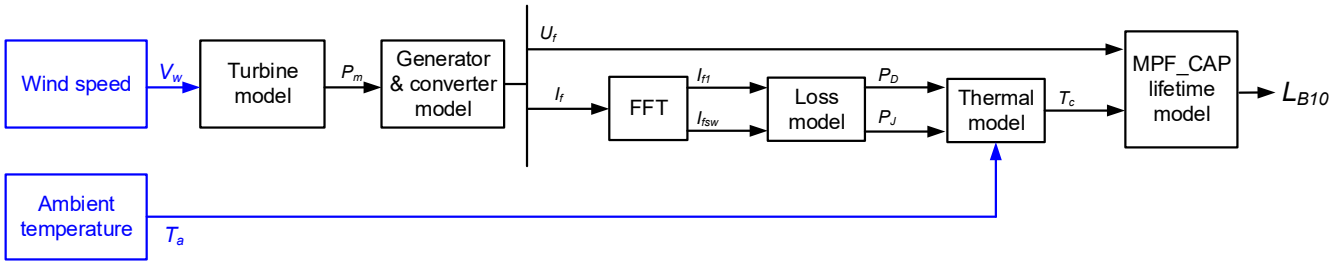

Fig. 9. Flowchart to calculate capacitor lifetime from mission profile.

According to the mission profile of the wind turbine system (e.g. wind speed and ambient temperature), the general procedure to calculate the lifetime of the capacitors is shown in Fig. 9. It can be seen that both the Joule power loss and dielectric power loss are taken into account in metalized polypropylene film capacitors (MPF-CAP) [13]. The lifetime model of the capacitor from the leading manufacturer is expressed as [14],

$$L_x = L_r \cdot \left(\frac{V_r}{V_x}\right)^{-n_1} \cdot 2^{\frac{T_r - T_x}{n_2}} \tag{2}$$

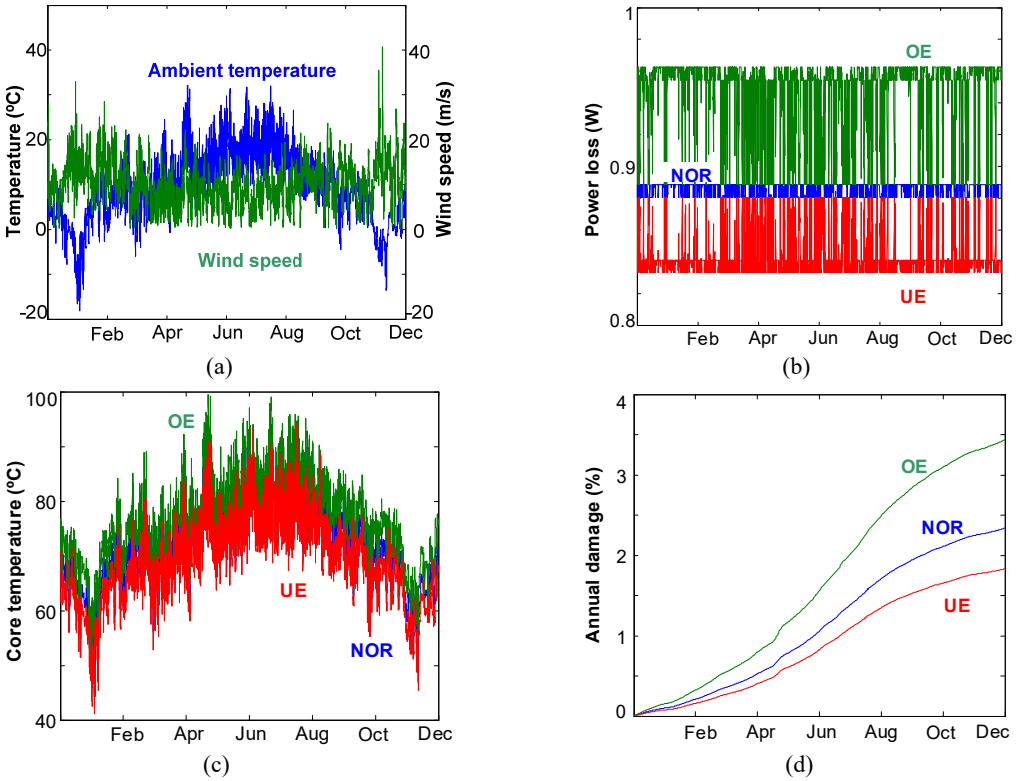

Fig. 10. Annual profile comparison at various operation modes. (a) Ambient temperature and wind speed; (b) Power loss profile; (c) Thermal stress profile; (d) Accumulated damage.

where L_x denotes the hours to failure at the applied voltage V_x and operational core temperature T_x, and L_r denotes the hours to failure at the rated voltage V_r and upper categorized temperature T_r. n_1 and n_2 are affecting coefficients of the voltage and temperature. It is noted that n_2 equals 10, and the n_1 equals 7 for the MPF-CAP [14].

With the annual wind speed (Class I) and ambient temperature with the sample rate of 1 hour as shown in Fig. 10(a), the loss profile, thermal profile and the annual accumulated damage are shown in Fig. 10(b), (c), (d), respectively. It can be seen that the supply of the reactive power changes the loss profile, thermal profile, and the lifetime expectancy of the LCL filter capacitor.

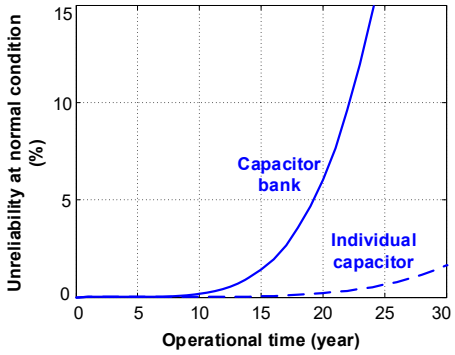

(a)

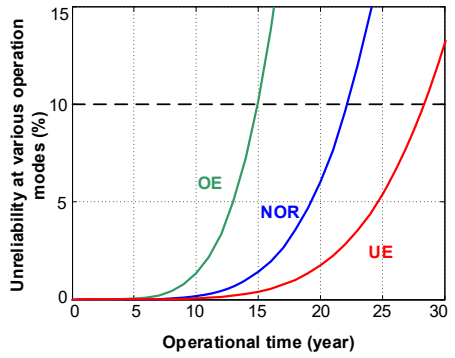

(b)

Fig. 11. Unreliability curve of the single capacitor and the capacitor bank. (a) From single capacitor to capacitor bank at normal condition; (b) Capacitor bank reliability at normal (NOR), over-excited (OE), and under-excited (UE) reactive power injection.

Since the same failure mechanism has the identical failure data distribution, the shape parameter of the Weibull distribution can be assumed at 5.13 for the MPF-CAP [6]. As any failure of the individual capacitor may result in the unreliable operation of the capacitor bank, all of the capacitors are connected in series in the reliability block diagram. The unreliability curve from the single capacitor to the capacitor bank is shown in Fig. 11. It can be seen that the B_{10} lifetime of the capacitor bank is significantly reduced due to a large amount of the used capacitors, where MPF-CAP bank lifetime is with of 22 years under the normal operation. Furthermore, the OE reactive power reduces the capacitor bank lifetime, while the UE reactive power increases the capacitor bank lifetime.

V. Conclusion

Aiming for the grid-connected inverter used in the renewable energy system, a reliability analysis method of the LCL filter capacitor is described in this paper. Based on the electrical stresses of the filter capacitor at different reactive power requirements, the percentile lifetime of the single capacitor can be predicted according to annual thermal profile. The Weibull function based time-to-failure distribution of the single capacitor can further be converted into the filter capacitor bank reliability by using the reliability block diagram. A system-level reliability study of 2 MW wind turbine system is analyzed and compared, considering whether the reactive power is supplied or not all year around. It is evident that the over-excited reactive power injection reduces the lifetime compared to no reactive power injection, while the under-excited reactive power slightly prolongs the lifetime.

References

[1] "ZVEI - Handbook for robustness validation of automotive electrical/electronic modules," Jun. 2013.

[2] D. Zhou, F. Blaabjerg, M. Lau, and M. Tonnes, "Optimized reactive power flow of DFIG power converters for better reliability performance considering grid codes," *IEEE Trans. on Industrial Electronics*, vol. 62, no. 3, pp. 1552-1562, Mar. 2015.

[3] K. Abdennadher, P. Venet, G. Rojat, J. M. Retif, and C. Rosset, "A realtime predictive-maintenance system of aluminum electrolytic capacitors used in uninterrupted power supplies," *IEEE Trans. on Industry Applications*, vol. 46, no. 4, pp. 1644–1652, Jul. 2010.

[4] A. Lahyani, P. Venet, G. Grellet, and P. J. Viverge, "Failure prediction of electrolytic capacitors during operation of a switch-mode power supply," *IEEE Trans. on Power Electronics*, vol. 13, no. 6, pp. 1199–1207, Nov. 1998.

[5] M. L. Gasperi, "Life prediction modeling of bus capacitors in ac variable frequency drives," *IEEE Trans. on Industry Applications*, vol. 41, no. 6, pp. 1430–1435, Nov. 2005.

[6] D. Zhou, H. Wang, and F. Blaabjerg, "Mission profile based system-level reliability analysis of DC/DC converters for a backup power application," *IEEE Trans. on Power Electronics*, vol. 33, no. 9, pp. 8030-8039, Sept. 2018.

[7] H. Oh, B. Han, P. McCluskey, C. Han, and B. D. Youn, "Physics-of-failure, condition monitoring, and prognostics of insulated gate bipolar transistor modules: a review," *IEEE Trans. on Power Electronics*, vol. 30, no. 5, pp. 2413-2426, May. 2015.

[8] L. Malesani, L. Rossetto, P. Tenti, and P. Tomasin, "AC/DC/AC PWM converter with reduced energy storage in the DC link," *IEEE Trans. on Industry Applications*, vol. 31, no. 2, pp. 287-292, Mar, 1995.

[9] E.ON-Netz. Requirements for offshore grid connections, Apr. 2008.

[10] M. Liserre, F. Blaabjerg, and S. Hansen, "Design and control of an LCL-filter-based three-phase active rectifier," *IEEE Trans. on Industry Applications*, vol. 41, no. 5, pp. 1281-1291, Sep. 2005.

[11] V. H. Prasad, "Analysis and comparison of space vector modulation schemes for three-leg and four-leg voltage source inverters," *Master dissertation*, Virginia Tech, Blacksburg, USA, 1997.

[12] D. Zhou, F. Blaabjerg, T. Franke, M. Tonnes, and M. Lau, "Comparison of wind power converter reliability with low-speed and medium-speed permanent-magnet synchronous generators," *IEEE Trans. on Industrial Electronics*, vol. 62, no. 10, pp. 6575-6584, Oct. 2015.

[13] "Aluminum Can Power Film Capacitors for PFC and AC Filter," KEMET datasheet, 2007.

[14] Capacitor lifetime calculator. (online: http://www.illinoiscapacitor.com/tech-center/life-calculators.aspx)